

ELECTRICAL RESPONSES OF RODS IN THE RETINA OF *BUFO MARINUS*

By L. CERVETTO, E. PASINO AND V. TORRE

*From the Laboratorio di Neurofisiologia del C.N.R., * Pisa,
Istituto di Scienze Fisiche, Genova and Laboratorio di Cibernetica
e Biofisica del C.N.R., Camogli, Italy*

(Received 2 April 1976)

SUMMARY

1. Intracellular responses to flashes and steps of light have been recorded from the outer segment and the cell body of rods in the retina of the *Bufo marinus*. The identification of the origin of recorded responses has been confirmed by intracellular marking.

2. Responses to flashes delivered in darkness or superimposed on a background were analysed. Responses recorded from outer segments conform to the principle of 'spectral univariance'. The shape of the response is not affected by enlarging the spot diameter from 150 to 1000 μm .

3. The membrane potential measured in darkness at the outer segments varied from -15 to -25 mV. Injection of steady hyperpolarizing currents increases the size of the response to light; depolarizing currents reduce the response. The mean value of the input resistance is 97 ± 30 M Ω in darkness and increases by 20–30% during illumination.

4. The responses obtained from the cell body of rods have the same shape, time course and spectral sensitivity of those recorded at the outer segment. Injection of steady current at the cell body produces different effects than at the outer segment: hyperpolarizing currents reduce the amplitude of the response to light; depolarizing currents increase the response.

5. The experimental data are fitted according to a model similar to that used to describe the responses of turtle cones (Baylor & Hodgkin, 1974; Baylor, Hodgkin & Lamb, 1974*a, b*).

6. The model reproduces the electrical responses of the rod outer segment to a variety of stimuli: (a) brief flashes and steps of light in dark adapted conditions; (b) bright flashes superimposed on background illuminations; (c) pairs of flashes delivered at different time intervals. Responses to hyperpolarizing steps of current are also reproduced by the model.

* The experiments have been carried out at the Laboratorio di Neurofisiologia del CNR, Via S. Zeno, 51, 56100 Pisa, Italy.

INTRODUCTION

Many observations indicate that hyperpolarizing responses to light of vertebrate photoreceptors are generated by a decrease in the permeability of the cell membrane to sodium ions (Hagins, Penn & Yoshikami, 1970; Zuckerman, 1971; Korenbrot & Cone, 1972; Cavaggioni, Sorbi & Turini, 1973; Cervetto, 1973; Brown & Pinto, 1974). An increase in the membrane resistance was measured in cones (Bortoff & Norton, 1967; Toyoda, Nosaki & Tomita, 1969; Baylor & Fuortes, 1970; Lasansky & Marchiafava, 1974) but not at the cell body of rods (Lasansky & Marchiafava, 1974). The deviation of the rod inner segment from the expected electrical behaviour may be explained by assuming that the outer segment is coupled to the cell body through a high axial resistance. Thus it is likely that the conductance changes measured at the cell body do not reflect those generated by light at the outer segment (Werblin, 1975).

We have investigated the functional properties of rods of *Bufo marinus* by analysing the intracellular responses to a variety of light and electrical stimuli. In the first part of the present paper experiments are described showing that light increases the membrane resistance at the outer segment although the membrane of the inner segment exhibits different electrical properties. In addition the absolute sensitivity and the temporal and spectral resolution of single rods are determined.

A theoretical analysis of the kinetics of rods photoresponses is worked out in the second part of this paper. The mathematical formulation of hypothesis that will be specified leads to equations reproducing the experimental results described in the first part of the paper. The model follows the general scheme of that proposed for describing the electrical responses of the cones of the turtle (Baylor *et al.* 1974*a, b*). Some of the previous hypothesis on the kinetics of cones have been modified to account for the different properties of the rod response.

METHODS

Preparation. The experiments were performed on retinae of the toad *Bufo marinus*. The animals were obtained from Drs W. De Rover, Reptielen-Amphibieen, Hertenaan 31D, Den Dolder, Holland. The eyes were removed from dark adapted animals and cut into anterior and posterior halves. After draining of the vitreous humour, the eyecup was mounted in a chamber where an oxygenated and buffered Ringer solution (in mM/l: Na⁺, 130; K⁺, 2.5; Cl⁻, 113; Ca⁺⁺, 1.5; Mg⁺⁺, 1.5; HCO₃⁻, 20; glucose, 5) flowed over the retina. The flow rate was kept constant at 4 ml./min and the temperature maintained at 20° C. The solution was saturated with 95% O₂ and 5% CO₂ by bubbling.

When penetrations were made from the receptor side, a portion of the retina was gently detached from the pigment epithelium, then inverted and secured to the

eyecup with a piece of filter paper. It is conceivable that with this procedure the outer segments of rods, instead of standing out straight, somehow fall over and lie obliquely on the plane of the retina. This may facilitate their penetration with micro-electrodes. The dissection of the retina was carried out under dim red light. The preparation was very stable and responses with normal amplitude and time course could be recorded after 7 hr. Before starting the measurements the eyecup was kept in complete darkness for at least half-an-hour.

Recording. Conventional glass micropipettes filled with 4 M potassium acetate were used for intracellular recordings. Their resistance, measured in the perfusing solution, was 200–400 M Ω . The activity was recorded via a negative capacitance pre-amplifier which also provided constant current for intracellular injection. During current injection, the voltage drop across the micro-electrode was balanced with a square pulse of opposite polarity and the capacitative component of the artifact was reduced by proper adjustments of the negative capacitance feed-back. In a large number of micro-electrodes current intensities higher than 2×10^{-10} A induced resistance changes which made balancing impossible (Frank & Fuortes, 1956). In these cases the data were discarded. The input resistance of rods was estimated from the slope of voltage-current curves measured in the range where the membrane behaved approximately linearly.

Light stimulation. The light source was a quartz-iodine lamp (Riluma 100W). The flux was split into two beams independently collimated; both illuminated a circular field aperture which could be given any one of a variety of diameters. The images of the two circular spots were combined by a beam splitter and focused on the retina. One of the two beams provided test flashes or steps of light, the other one constant backgrounds. Flashes and steps of light of different durations (specified in the text) were obtained by driving an electromagnetic shutter. The actual wave form of the light stimuli impinging on the retina was monitored by a photocell. The rising time of the stimuli was less than 1 msec. The total energy of the unattenuated light with wave-lengths between 450 and 900 nm was about 2.5×10^3 erg. cm $^{-2}$. sec $^{-1}$. Neutral density filters provided the desired light attenuation. In order to determine the spectral sensitivity of rod responses, narrow bandwidth interference filters (half-widths about 20 nm) were inserted on the collimated beams. The filters transmittance was measured with a silicon photodiode with flat spectral response in the range between 450 and 960 nm within an error of 7%. The spectral energy distribution of the source was derived and the irradiance values converted in photon. cm $^{-2}$. sec $^{-1}$ were: 5.69×10^{10} at 470 nm; 1.54×10^{11} at 510 nm; 2.66×10^{11} at 550 nm; 7.14×10^{11} at 590 nm; 1.52×10^{12} at 630 nm; 2.43×10^{11} at 670 nm.

Identification of the recorded responses. Responses of rods were easily distinguishable from graded potentials recorded from other cells because of their different time course. Recordings from the outer segment of rods were obtained by approaching the retina from the receptor side; in this case the penetration of the cell occurred as soon as the electrode touched the retina. Penetrations of rods at the cell body were accomplished by approaching the retina from the vitreal surface. In these conditions the impalement of the rods occurred immediately after penetration of a horizontal cell.

More conclusive evidence about the origin of a particular kind of response was obtained from experiments in which iontophoretic injections of Procion yellow were made. This method also served to establish whether the responses were recorded at the outer segment or at the cell body of the rods. The micropipettes were filled with a 5% aqueous solution of Procion yellow MAR 4. The dye was injected by passing square pulses of inwardly directed current 10^{-9} A in amplitude and 0.5 sec in duration, at 1 sec interval for 7 min. In many instances responses could be recorded at the end of injection. Fixation of the retina was delayed for at least half-an-hour after the

injection, to allow dye diffusion within the cell. In order to limit the diffusion of the dye to the cell region close to the electrode penetration, retinae were promptly fixed at the end of injection with 5% formaldehyde flowing through the perfusion chamber for 15 min. Typical results are shown in Pl. 1.

RESULTS

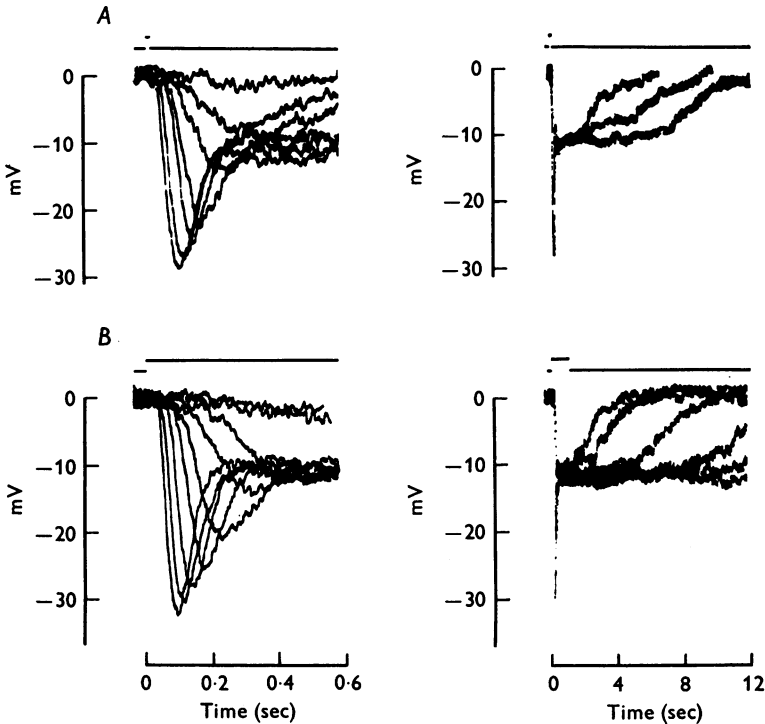
The toad retina contains different classes of photoreceptors with distinct morphologies (Walls, 1963) and absorbing pigments (Crescitelli, 1972; Hárosi, 1975). In the present experiments, we mostly encountered one class of rods with the greatest sensitivity at about 510 nm. In one instance we observed a cell with a maximal sensitivity at wave-lengths shorter than 470 nm. The striking predominance of one class of cells may in part reflect the fact that in the *Bufo* retina *red* rods predominate in number over the *green* rods and over cones. Other reasons, however, like different sizes and shapes of outer segments and cell bodies or a selective topographical distribution within the retina should also be considered.

Graded hyperpolarizing responses to light were recorded intracellularly following penetration of the retina from the receptor side. The membrane potential measured in darkness upon withdrawal of the micro-electrode ranged between -15 and -20 mV. The potential change evoked by bright light often exceeded -30 mV; only rods with maximal responses exceeding -20 mV were considered in the present study. Histological controls after injections of Procion dye revealed that the majority of responses originated at the outer segment of rods (Pl. 1).

Responses to flashes and steps of white light

The responses of a rod to flashes and steps of increasing intensities are illustrated in Text-fig. 1, at two different time scales. For dim flashes the potential reaches a peak in about 0.35 sec while for the brightest flashes the time to peak is reduced to less than 0.1 sec. After reaching the peak of the response to bright flashes, the membrane potential quickly drifts to a less negative plateau of about 12 mV and maintains it for several seconds. The plateau saturates at light intensities weaker than those saturating the peak. The membrane potential decays to the resting level with distinct time constants depending on the intensity and duration of light. Responses to dim flashes decay with a time constant of about 0.2 sec (τ_1), while responses to bright flashes decay from the plateau with a time constant of about 1 sec (τ_2). The duration of the plateau increases with the intensity of the light: with very bright steps the plateau lasts up to 20 sec and the membrane potential decays to the resting level with a time constant of approximately 4 sec (τ_3). These observations confirm

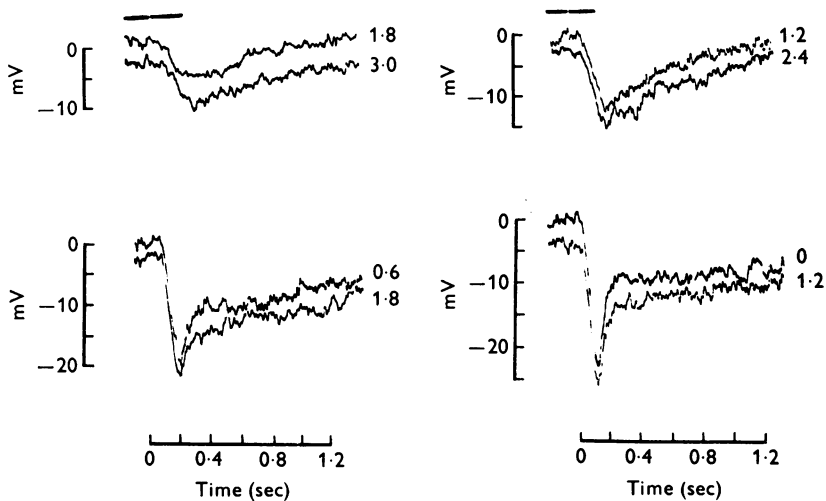
previous studies (Toyoda, Hashimoto, Anno & Tomita, 1970; Schwartz, 1973; Baylor & Hodgkin, 1973; Lasansky & Marchiafava, 1974) indicating that light responses of rods and cones have different time courses. In particular, the time constant of decay is considerably longer in rods than in cones.



Text-fig. 1. *A*, rod responses to 13 msec flashes and *B*, to 1 sec steps of white light at different intensities. The stimulus was a circular spot of diameter $1000 \mu\text{m}$. Responses are shown at two different time scales. *A*, flashes: responses at the fast time scale were obtained with light intensity attenuations varying from 3.6 to 0 log. units; on slower time scale responses to 1.2, 0.6, 0 log. units attenuated flashes are shown. *B*, steps: responses at the fast time scale were obtained with light attenuations varying from 5.4 to 0.6 log. units; on the slower time scale, responses to attenuated lights from 3.6 to 0.6 log. units are shown. The unattenuated light was equivalent to a 510 nm monochromatic light with intensity 2.8×10^4 photons $\cdot \mu\text{m}^{-2} \cdot \text{sec}^{-1}$. The zero level of membrane potential is arbitrary and indicates the level of membrane potential in darkness.

Text-fig. 2 shows the responses of a rod to spots of two different diameters, 150 and $700 \mu\text{m}$, respectively. In the case illustrated, the responses produced by the small spot match over the entire range of intensities the responses obtained with the large spot with intensities

reduced by 1.2 log. units. The average shift in intensity, however, was of 0.9 log. units. The enhancement of the responses to the large spot could be due to the electrical coupling between rods (Copenhagen & Owen, 1976). A drop in the effective intensity of smaller spots, due to poor focusing, may also partially account for the effect.



Text-fig. 2. Comparison of responses to small ($150\ \mu\text{m}$) (upper trace) and large ($700\ \mu\text{m}$) spot (lower trace) at different light intensities. The light attenuation in log. units is indicated to the right of each record.

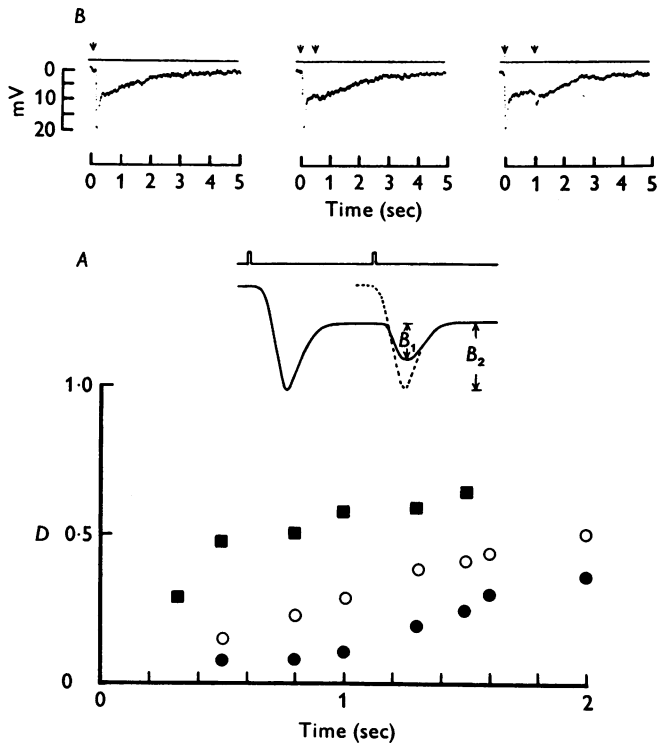
Temporal resolution of rod responses

We studied the temporal resolution in rods by analysing their responses to paired flashes. The intensities of the two flashes were kept equal while varying the time interval (Δt) between the two stimuli. For Δt less than 50 msec the combined response to paired stimuli was similar to that evoked by a single flash of double intensity. For Δt higher than 50 msec the duration of the response was increased and a second peak eventually appeared. By increasing the intensity of the paired flashes the second peak appeared at Δt progressively longer (Text-fig. 3). A way to characterize these effects is to consider the quantity

$$D = \frac{B_1}{B_2},$$

where B_1 and B_2 are potential changes measured from the plateau. B_1 is the actual amplitude of the response produced by the second flash. B_2 indicates the amplitude of a potential change reaching the same absolute level of hyperpolarization as the response to the first flash. The quantity D is plotted in Text-fig. 3 as a function of Δt for three intensities of light. For weak and moderate flashes ($V_1/V_{\text{max}} = 0.51$ and $V_1/V_{\text{max}} = 0.78$

respectively, where V_1 is the measured peak amplitude and V_{\max} the peak amplitude to the brightest flash), a second peak is present when Δt is greater than 300–400 msec. For bright flashes ($V_1/V_{\max} = 0.98$) a second peak is barely detectable for Δt around 0.5 sec and is clearly present when Δt is greater than 1 sec.

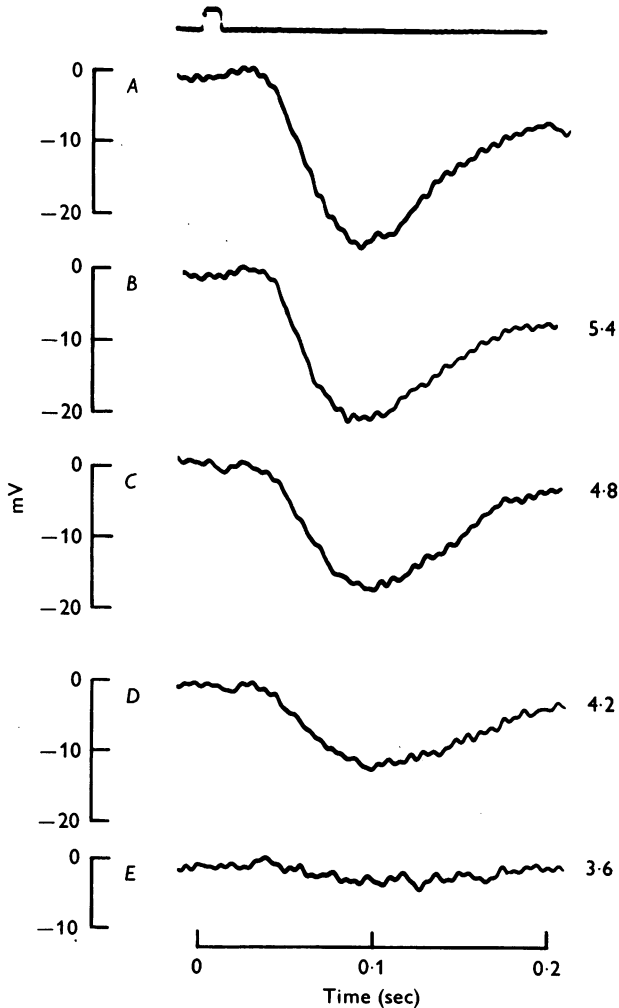


Text-fig. 3. *A*, plot of the quantity D as a function of the time interval (Δt) between the flashes of the pairs. The quantity on the ordinates represent the ratio B_1/B_2 where B_1 and B_2 are the peak amplitudes shown in the insert. The relation between D and Δt is plotted for three values of light intensity. The light intensity is expressed in log. units of attenuation: 1.8, ■; 1.2, ○; and 0.6, ●. *B*, starting from the left, is the record of the response to a single flash and to paired flashes delivered at time intervals 0.5 and 1 sec respectively.

Effect of background illumination on responses to flashes

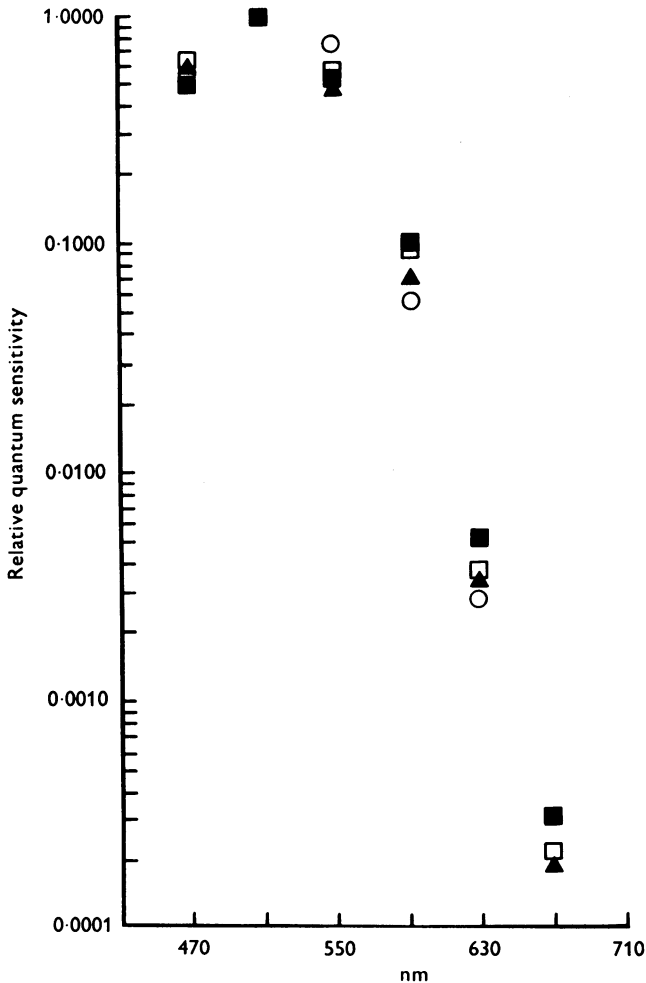
The following experiments describe the action of steady illumination of different intensities on the responses to flashes. The analysis was limited to the effect of background illuminations initiated 1 sec before the presentation of the text flash, as at this time the response to the background has reached a steady state. Text-fig. 4 shows for comparison the

response to a bright flash presented in darkness (Text fig. 4 *A*) and superimposed on background illuminations of four different intensities covering a range of about 2 log. units. The most evident consequence of the steady illumination is to reduce the amplitude of the response to the test flash. This is consistent with previous observations in both invertebrate (Fuortes & Hodgkin, 1964) and vertebrate photoreceptors (Baylor & Hodgkin,



Text-fig. 4. Effect of background illumination on responses to a flash of fixed intensity. *A*, is the response to the flash without background illumination. *B-E*, are the responses to the same flash delivered in the presence of background illumination of different intensities. Numbers at the right of records indicate the log. units of light attenuation of the background.

1974). In our experimental conditions, however, as the intensity of the steady background was raised, the time to peak increased slightly. In considering possible explanations, it is important to note that the shortening of the time to peak with flashes of increasing intensity is more evident in rod than in cone responses. It is conceivable that in certain experimental conditions the presence of a background saturates the mechanism responsible for the shift of the peak. The same effect has been observed also in cones with very bright background illuminations (Baylor & Hodgkin, 1974).



Text-fig. 5. Spectral sensitivity of four rods penetrated at the outer segment. The ordinate is relative quantum sensitivity; the abscissa, wave-length. All cells have a peak sensitivity at about 510 nm.

Spectral sensitivity

Spectral sensitivity was determined by plotting the relative quantum sensitivity as a function of the wave-length, using an amplitude criterion of 1.5 mV. The results collected from four rods are shown in Text-fig. 5. The curves from individual rods fall into a single group with peak sensitivity at about 510 nm. This corresponds to the value determined by spectrophotometric measures in the red rods of *Bufo marinus* (Hárosi, 1975). With appropriate adjustment of light intensity, responses to flashes of different wave-lengths have the same time course indicating that the rods of *Bufo marinus* signal the absorbed light independently of wave-length, thus obeying the principle of spectral univariance (Naka & Rushton, 1966). This observation seems in contradiction with results reported by Schwartz (1975) in the turtle. It is possible, however, that interactions between cones and rods occur at the cell body and cannot be detected in the outer segment.

Absolute sensitivity

The measurements of absolute sensitivity were obtained with spots of monochromatic light covering large areas; in these conditions, the pool of interacting rods is expected to be isopotential and the responses may be considered as obtained from isolated rods.

The effective collecting area A_c (Baylor & Hodgkin, 1973) is the geometrical collecting area A_g corrected for the effective light absorbed in the outer segment. Following Baylor & Hodgkin (1973):

$$A_c = A_g \phi(1 - T(\lambda)),$$

where ϕ is the quantum efficiency and $T(\lambda)$ is the transmittance of the outer segment of the receptor. From Lambert's law $T(\lambda) = 10^{-a(\lambda)l}$, where $a(\lambda)$ is the absorptivity and l is the length of the outer segment. The absorptivity at the optimum wave-length has values around $1.5 \times 10^{-2} \mu\text{m}$ (Rodieck, 1973). The geometrical collecting area may be assumed $50 \mu\text{m}^2$ and the average length of the outer segment $51.3 \mu\text{m}$ (Hárosi, 1975). The quantum efficiency ϕ of rods is 0.68 in the frog (Dartnall, 1968). With these numerical values, A_c is equal to $28 \mu\text{m}^2$.

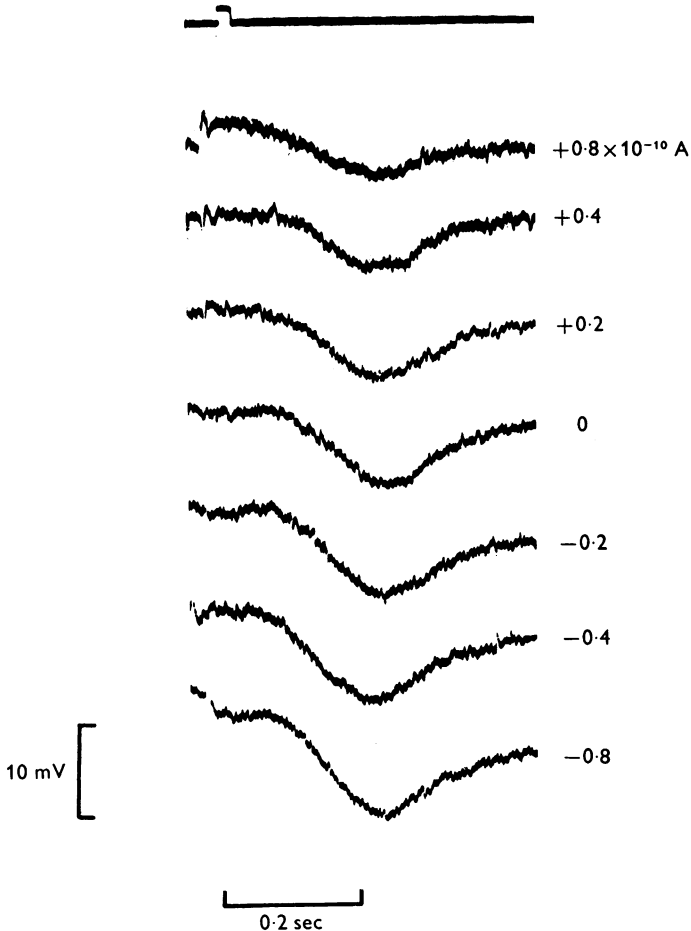
Thus the absolute sensitivity is:

$$\sigma = \frac{V_{\text{peak}}}{IA_c \Delta t},$$

where V_{peak} is the peak hyperpolarization for very weak flashes, I is the intensity of the light and Δt is the flash duration. At 510 nm, σ has values between 400 and $650 \mu\text{V}$ per photoisomerization per receptor. Similar values have been reported by Fain (1975).

Electrical properties of the membrane of rod outer segments

The input resistance of the membrane of the rod outer segment was derived from the linear slope of current-voltage characteristics obtained by injecting either short (30 msec) or longer steps (400 msec) of current.

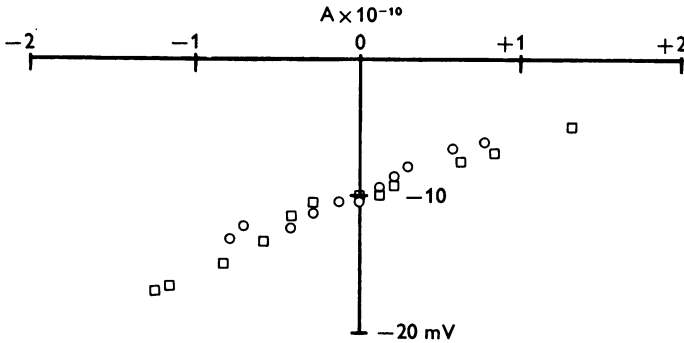


Text-fig. 6. Effect of polarization of the membrane of an outer segment upon the response to a flash. Figures at the right indicate the intensity and polarity of the polarizing currents. The middle record, indicated with 0, is the response to the flash in the absence of extrinsic current. Postive current is outward, negative current inward.

Reliable measurements of the effect of current on the cell membrane could be obtained only with intensities not exceeding 1.5×10^{-10} A. Stronger currents usually produced changes in the micro-pipette which masked the behaviour of the membrane. Currents weaker than 0.5×10^{-10} A

symmetrically depolarize or hyperpolarize the rod membrane with a time constant of about 6 msec. Stronger currents produce voltage and time dependent rectification. The mean values of membrane resistance and time constant calculated in fifteen cells were $97 \pm 30 \text{ M}\Omega$ and $6 \pm 0.5 \text{ msec}$, respectively.

Text-fig. 6 shows the responses to a flash of moderate intensity superimposed on various levels of polarization of the membrane. It is shown that the light response is reduced during the injection of weak depolarizing

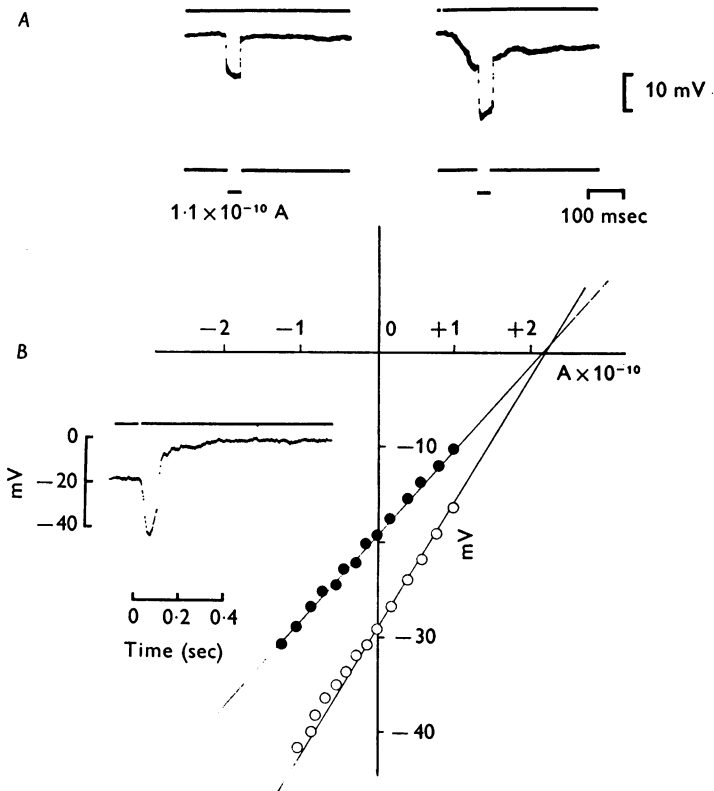


Text-fig. 7. Plot of the peak amplitudes of light responses as a function of currents injected through the micro-electrode. Symbols indicate two different cells. Both cells show a resistance increase of about $40 \text{ M}\Omega$.

currents, while it is enhanced by hyperpolarizing currents. The peak amplitude of the photoresponses of two rods is plotted in Text-fig. 7 as a function of the intensity of the polarizing currents. The relation is approximately linear in the range of currents used. The slope of the straight line may be taken as an indication that the membrane resistance increases by about $40 \text{ M}\Omega$ during the response to light.

As already shown in photoreceptors of different animals (Baylor & Fuortes, 1970; Lasansky & Marchiafava, 1974) the comparison between the voltage-current characteristics in darkness and during illumination gives indication of the conductance changes responsible for the photoresponse. Text-fig. 8 illustrates an example of a similar experiment performed on the outer segment of a rod of *Bufo marinus*. The voltage drop produced by a 30 msec pulse of negative current is shown both in darkness and at peak of the photoresponse (Text-fig. 8A). The voltage current characteristics obtained from the same cell in darkness and at the peak of the response to light are shown in Text-fig. 8B. The experimental points can be fitted by straight lines whose slope is $91 \text{ M}\Omega$ in darkness and $133 \text{ M}\Omega$ at the peak of the photoresponse. The extrapolated intersection of the two curves gives a value of reversal potential near zero absolute of membrane

potential. This result is similar to those obtained in the cones of turtle (Baylor & Fuortes, 1970) and salamander (Lasansky & Marchiafava, 1974). This suggests that similar conductance changes are initiated by light in both cones and rods.



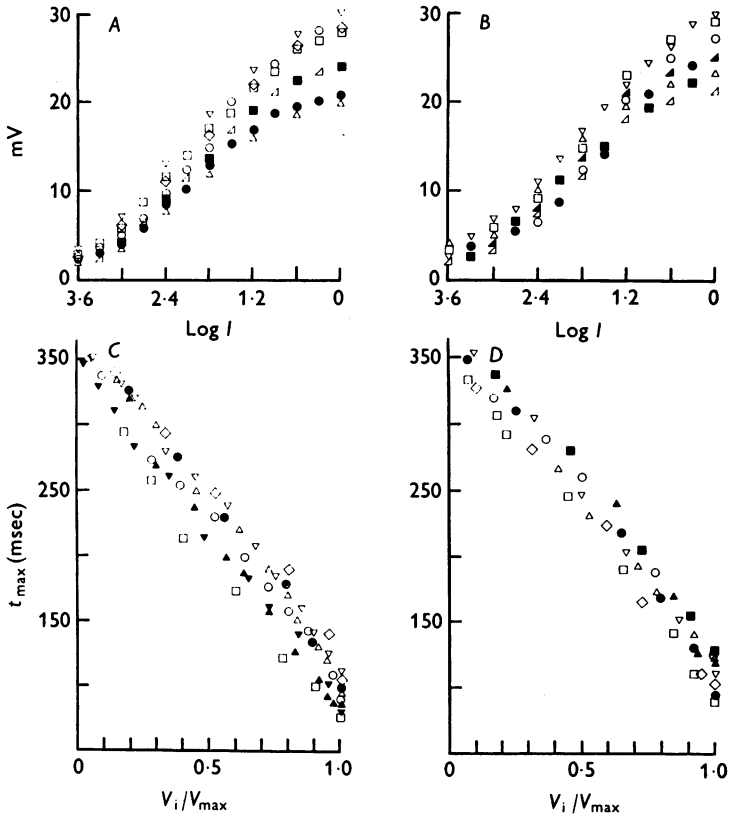
Text-fig. 8. Voltage-current characteristics of the outer segment of a rod obtained with short pulses of current delivered in darkness and at the peak of the photoresponse. *A*, records of the voltage drop produced by a 1.1×10^{-10} A pulse of current in darkness and at the peak of the photoresponse. *B*, voltage-current characteristics of the same rod in darkness (●) and at the peak of the response to light (○). The inset illustrates the membrane potential of the same cell as a potential shift observed at the end of a light response when the micro-electrode accidentally moved out of the cell. The slopes of the straight lines fitting the data correspond to an input resistance of ≈ 91 M Ω in darkness and 133 M Ω at the peak of the response to light. The lines intersect at $\approx +2$ mV.

Photoresponses measured at the cell body

Responses recorded from the cell body have amplitude and time course similar to those obtained from other cells penetrated at the outer segment. The amplitude (V_1) and time to peak (t_{\max}) of the response obtained from

rods penetrated at the two different cell regions are compared in Text-fig. 9. The relation between V_i and $\log I$ is plotted for eight rods penetrated at the outer segment (Text-fig. 9A) and at the cell body (B). Plots of the time to peak against V_i/V_{\max} are also shown in Text-fig. 9C (outer segments) and in D (cell body). No significant difference is observed between the two series of results.

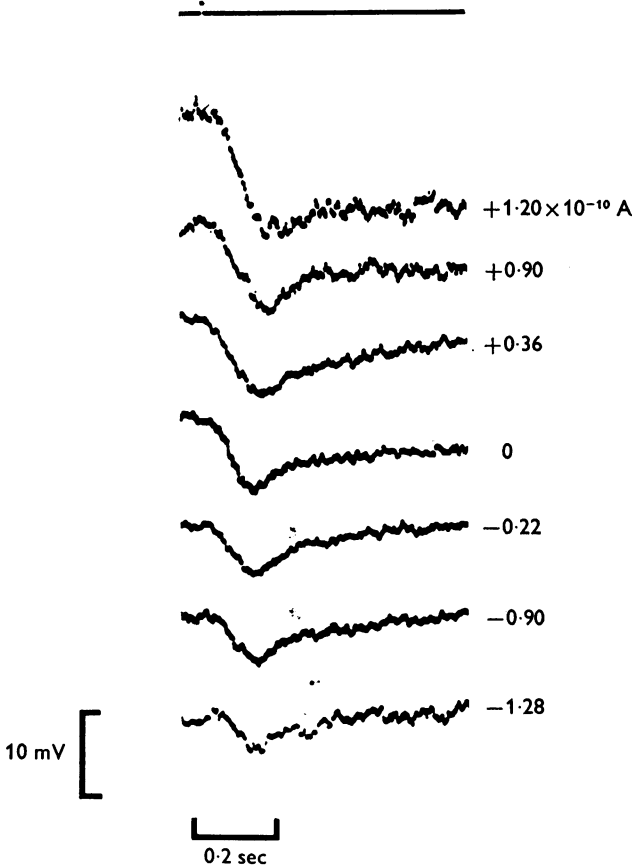
The spectral sensitivity measured in rods penetrated from the vitreal side also resembles that obtained from visual cell penetrated at the outer segment.



Text-fig. 9. Amplitude intensity and time to peak characteristics for rods penetrated at the outer segment (A, C) and at the cell body (B, D). A, plot of responses obtained from eight different outer segments. B, same as in A, for eight different rods penetrated at the cell body. Both in A and B, data superimpose without any shift along the abscissa. C, relations between time to peak and normalized amplitude response in eight outer segments. D, same as in C, for eight rods penetrated at the cell body. The flash duration is 13 msec.

Effects of injected currents at the cell body

The effect of current injection on the photoresponse obtained from the cell body is shown in Text-fig. 10. Here the hyperpolarizing currents progressively reduce the amplitude and accelerate the time course of the photoresponse, while depolarizing currents significantly increase the



Text-fig. 10. Effects of steady currents on light responses of a rod penetrated at the cell body. Figures at the right indicate the intensity and polarity of the polarizing currents. The middle record, indicated with 0, is the light response in absence of extrinsic current.

amplitude and the duration of the light response. These results are consistent with the data reported by Lasansky & Marchiafava (1974) on the rods of *Ambystoma tigrinum*.

As a plausible explanation for the differences observed between outer

segment and cell body, it has been suggested that the two regions of the visual cell are coupled by a high axial resistance (Werblin, 1975). Accordingly, the conductance changes observed at the cell body would not reflect those generated by light but would originate from a voltage dependent process initiated by the hyperpolarization of the outer segment. However, the observation that photoresponses originating from outer and inner segment have similar amplitude and time course requires that such regenerative mechanism amplifies the signal without any appreciable delay and distortion.

Analysis of the responses of rods

A detailed theoretical analysis of the photoresponses of turtle cones has been recently given (Baylor & Hodgkin, 1974; Baylor *et al.* 1974*a, b*). It is supposed that light starts a chain of linear reactions leading to the appearance of a substance, (Z_1), which blocks ionic channels, thereby generating the hyperpolarizing response. The blocking substance is degraded through a series of successive reactions with distinct rate constants. To account for the shortening of time to peak of the response to lights of increasing intensity it has been supposed that blocking molecules are reversibly converted to an inactive substance (Z_2) by an autocatalytic reaction. The sag of potential from the peak to the plateau has been ascribed to a voltage and time dependent conductance.

In the following sections we propose a model for the rods of *Bufo marinus* which retains the basic concepts of the model of Baylor *et al.* (1974*b*) but introduces some changes to account for the peculiarities of rod responses described in the Results. Here the sag of potential from a peak of 20–32 mV to a plateau of 7–12 mV is attributed to desensitization of the light dependent conductance while the voltage and time dependent conductance merely accelerates the sag. The desensitization of the light dependent conductance is obtained in our model, by assuming that the reaction from Z_2 into Z_1 is controlled by an enzyme. It follows that the rate of reaction from Z_2 to Z_1 is limited by the available enzyme while the rate of reaction from Z_1 to Z_2 can increase indefinitely with the concentration of Z_2 . The mathematical formulation of these hypotheses leads to equations reproducing the responses of the rod outer segment to flashes and steps of light.

Determination of dark parameters

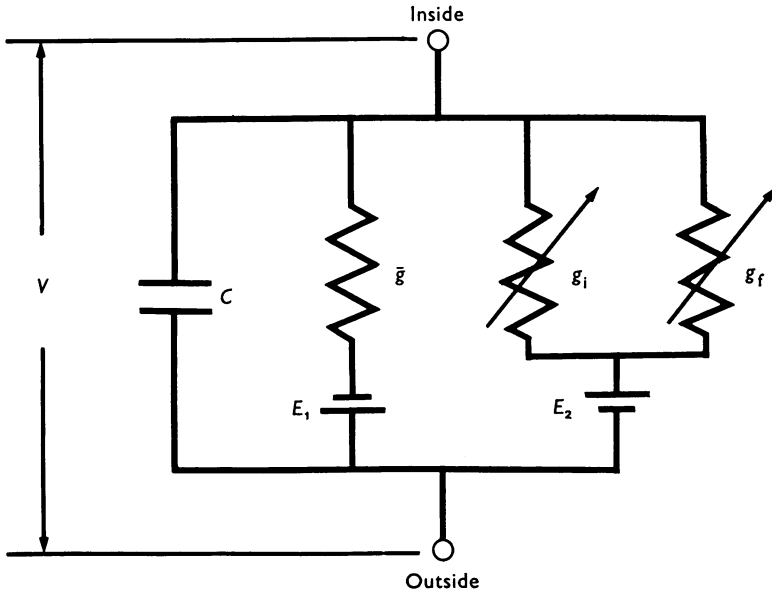
Text-fig. 11 shows the equivalent electrical circuit of the membrane of the rod outer segment. C is the membrane capacity; \bar{g} is a fixed conductance in series with the battery E_1 ; g_2 and g_1 are two conductances in series with the battery E_2 ; g_1 is the light sensitive conductance and g_2 is a voltage and time dependent conductance, having in darkness (–18 mV) a value near 0.

The differential equation of the circuit is:

$$C \frac{dV}{dt} = \bar{g}(E_1 - V) + (g_i + g_f)(E_2 - V), \quad (1)$$

where V is the membrane potential.

We suppose that, as in turtle cones (Baylor *et al.* 1974*a,b*), absorption of photons by the pigment molecules of rods leads to the release of a diffusible substance, Z_1 , which interacts with selective ionic channels and by reducing the conductance g_i hyperpolarizes the cell membrane.



Text-fig. 11. Equivalent circuit of the membrane of rod outer segment. C is the membrane capacity, \bar{g} is a fixed conductance in series with the battery E_1 which limits the maximal amplitude of the light response. The two conductances g_i and g_f are in series with the battery E_2 . g_i is the light sensitive conductance and g_f is a voltage and time dependent conductance.

Assuming that the concentration of free Z_1 always greatly exceeds the concentration of bound Z_1 , and that both binding and release reactions are sufficiently rapid to reach instantaneously a near equilibrium condition, then:

$$g_i = \frac{\bar{g}_i}{1 + (z_1/K)}, \quad (2)$$

where \bar{g}_i is the value of g_i when $z_1 \sim 0$, a condition which is assumed to be approached in darkness and K is the dissociation constant as in Baylor *et al.* (1974*b*).

The extrapolated value of the reversal potential (see Text-fig. 8) for the response is close to +2 mV thus indicating a value for the battery E_2 close to zero. The value assigned to the battery E_1 is -60 mV which corresponds to the absolute level of hyperpolarization approached by maximal light responses.

In darkness $g_t \sim 0$ and the input resistance of the cell is 91 M Ω .

Thus:

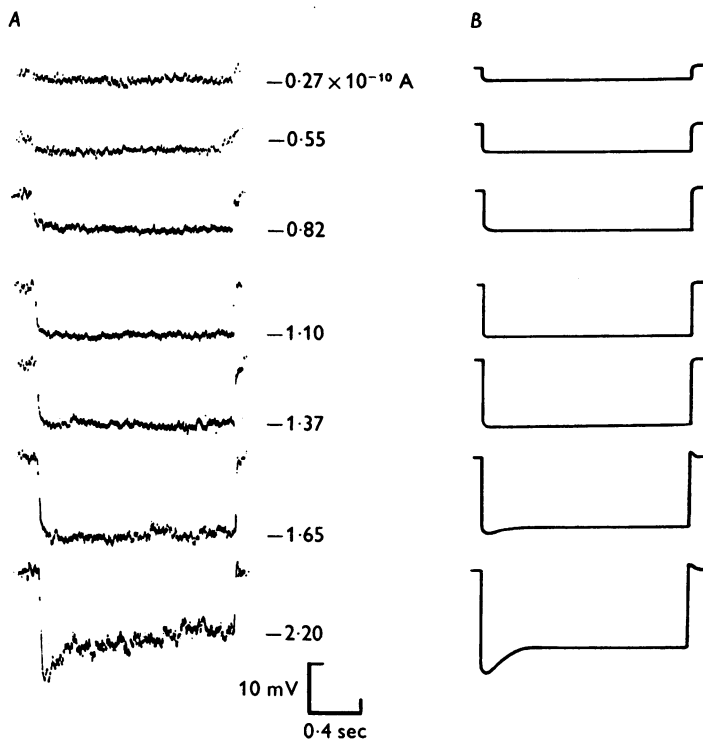
$$\bar{g}_1 + \bar{g} = 110 \times 10^{-10} \text{ mho}, \quad (3)$$

$$\frac{\bar{g} E_1}{\bar{g} + \bar{g}_1} = -18 \text{ mV},$$

and solving:

$$\bar{g} = 33 \times 10^{-10} \text{ mho}, \quad \bar{g}_1 = 77 \times 10^{-10} \text{ mho}.$$

The mean values of input resistance and time constant give for the membrane capacity a mean value of 62 pF.



Text-fig. 12. *A*, effect of steady hyperpolarizing currents on the membrane of a rod and *B*, responses computed from the model based on the equations for the equivalent circuit and with the parameters reported in Tables 1 and 2. The value of the currents is given by the numbers in the middle.

Determination of the voltage dependent conductance

Text-fig. 12*A* shows the voltage deflexions produced by steady hyperpolarizing currents across the membrane of the outer segment. It is seen that the membrane is ohmic for currents up to 1.2×10^{-10} A. A delayed rectification appears with currents greater than 1.7×10^{-10} A.

Such modification is attributed to the voltage and time dependent conductance g_t which can be empirically described by equations similar to those used to character-

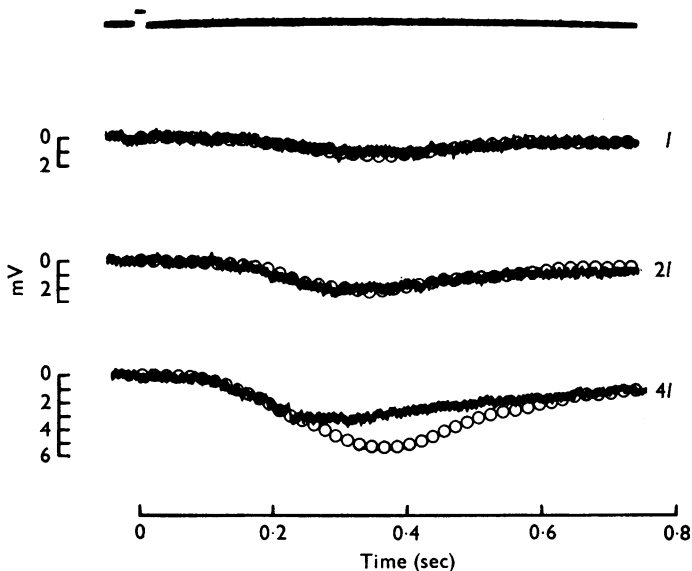
ize ionic conductances in the nerve membrane (Hodgkin & Huxley, 1952) and in the cardiac Purkinje fibres (McAllister, Noble & Tsien, 1975).

The curves in Text-fig. 12*B*, yielding a fair reproduction of the experimental data (Text-fig. 12*A*), were obtained theoretically assuming the following equations:

$$g_t = \bar{g}_t h^3, \quad (4)$$

$$\frac{dh}{dt} = \frac{h_\infty(V) - h}{\tau_h(V)}, \quad 0 \leq h \leq 1, \quad (5)$$

with $\bar{g}_t = 4.95 \times 10^{-9}$ mho and using the functions $h_\infty(V)$ and $\tau_h(V)$ given in Table 1.

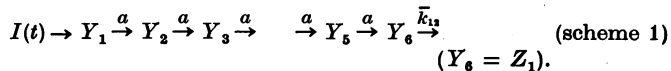


Text-fig. 13. Linearity of response of a rod to weak flashes of white light. Numbers on the right indicate the light intensity in relative units. The circles superimposed to the first record were obtained from eqns. (1) and (2) with the numerical values indicated in the text assuming that with dim flashes $z_1/K \ll 1$ so that $g_t \sim \bar{g}_t (1 - z_1/K)$. The circles superimposed to the other records were obtained by multiplying the fitting of the first record by a factor proportional to the light intensity. Linearity holds only for responses below 2–2.5 mV.

Linear responses to flashes

Text-fig. 13 shows the responses of a rod to three weak flashes of relative intensities I , $2I$, $4I$. It is seen that linearity fails for hyperpolarizations greater than 2–2.5 mV.

The circles represent the responses computed according to eqns. (1) and (2) assuming that the particles Z_1 are built up through a chain of six linear reactions represented by scheme (1) with $\alpha = 16 \text{ sec}^{-1}$ and $\bar{k}_{12} = 10 \text{ sec}^{-1}$.



Linear responses could be well fitted according to scheme (1) in the majority of the cells. However, the particular values of the parameters α and \bar{k}_{12} given above were not applicable to all of the recorded cells.

Nature of the plateau

The rods of *Bufo marinus* respond to strong flashes and steps of light with a hyperpolarization which quickly drifts from a peak of about -30 mV, to a plateau of about -12 mV maintained for several seconds.

The sag of the potential from the peak to the plateau may be explained by either the effect of a voltage and time dependent conductance (Baylor *et al.* 1974*a*) or a desensitization of the light sensitive conductance as in the ventral photoreceptor of *Limulus* (Millecchia & Mauro, 1969*a, b*) and in the eye of *Balanus* (Brown, Hagiwara, Koike & Meech, 1970).

In rods of *Bufo marinus* the plateau stabilizes at levels of potential within the range of the ohmic behaviour of the membrane (Text-fig. 12*A*). If the plateau were due to the effect of the voltage and time dependent conductance g_t , weak steps of current, superimposed on the plateau, should reveal a time dependent rectification. In experiments where steps of current were injected during the plateau, no time dependent rectification was observed for hyperpolarizing currents of intensities up to $0.3-0.5 \times 10^{-10}$ A; higher intensities induced delayed rectification. These results indicate that g_t is negligible during the plateau while it increases with additional hyperpolarization. Accordingly, the equations characterizing g_t with the parameters given in Table 2, show that at the plateau, 1 sec after the peak $g_t \simeq 0$.

Desensitization of the light dependent conductance

The aim of the present section is to show that the model proposed by Baylor *et al.* (1974*a, b*) for the degradation of Z_1 into the products Z_2, Z_3 , etc., can account for our data on *Bufo* rods only if the ratio k_{12}/k_{21} (see reference) is not constant. This leads to the assumptions concerning the desensitization of g_t (see Text-fig. 17). For this we analyse the plateau of responses to both steps and bright flashes.

Responses to bright flashes, 10 msec duration, are illustrated in Text-fig. 14. The ratio z_1/K at the plateau can be derived in terms of electrical quantities from eqns. (1) and (2) taking into account that both g_t and \dot{V} are negligible. By considering that $E_2 = 0$, we obtain the simple relation:

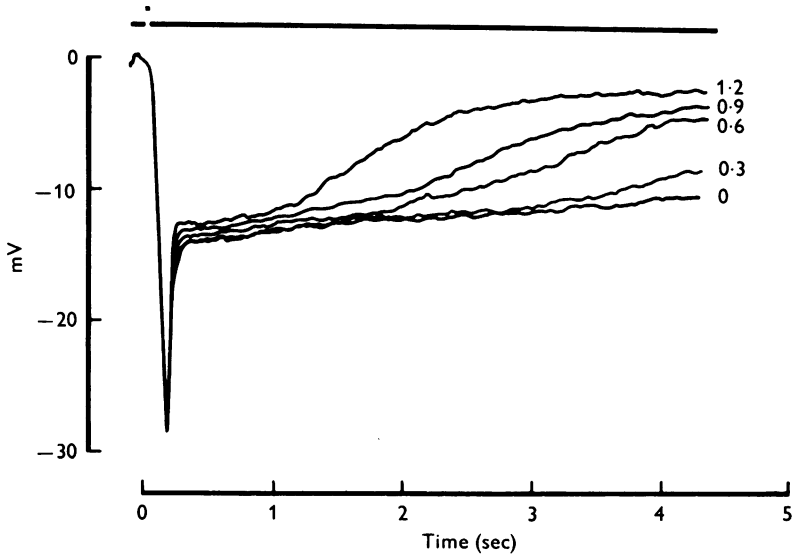
$$\frac{z_1}{K} = \frac{V - V_D}{V_D - aV}, \quad a = \frac{\bar{g}}{g_1 + \bar{g}}, \quad (6)$$

where V_D is the membrane potential in darkness.

From the scheme (1) with $\alpha = 16 \text{ sec}^{-1}$ and $\bar{k}_{12} = 10 \text{ sec}^{-1}$ it results that the production of the substance Y_6 ($= Z_1$) stops about 1.2 sec after the

onset of light. Thus, since at this time V is nearly constant, it follows that both Z_1 and Z_2 are also nearly constant and their concentrations are related by:

$$z_1 = \frac{k_{21}}{k_{12}} z_2 = \bar{C} z_2. \quad (7)$$



Text-fig. 14. Plateau in the response to bright flashes. Five tracings from responses to 10 msec flashes of white light of increasing intensity. Numbers on the right give the values of light intensity attenuation in log. units. After the peak of the response (25–28 mV) a plateau is reached (12–13 mV), and it is maintained for several seconds.

Furthermore, since the non-linearities of the process shown in scheme (2) (see p. 40) influence only the conversion from Z_1 to Z_2 in both forward and backward directions (cf. also Baylor *et al.* 1974*b*), we have:

$$z_1 + z_2 \simeq FI\Delta t, \quad (8)$$

where I is the flash intensity, Δt the flash duration and F a constant. From eqns. (7) and (8):

$$\frac{z_1}{K} = MI; \quad M = \frac{\bar{C}F\Delta t}{K(1+\bar{C})}. \quad (9)$$

The values of z_1/K are obtained from the data shown in Text-fig. 14 with eqn. (6) and plotted against the light intensity in Text-fig. 15. It is obvious that the experimental points cannot be fitted by a straight line through the origin as predicted by eqn. (9) assuming $\bar{C} = \text{constant}$.

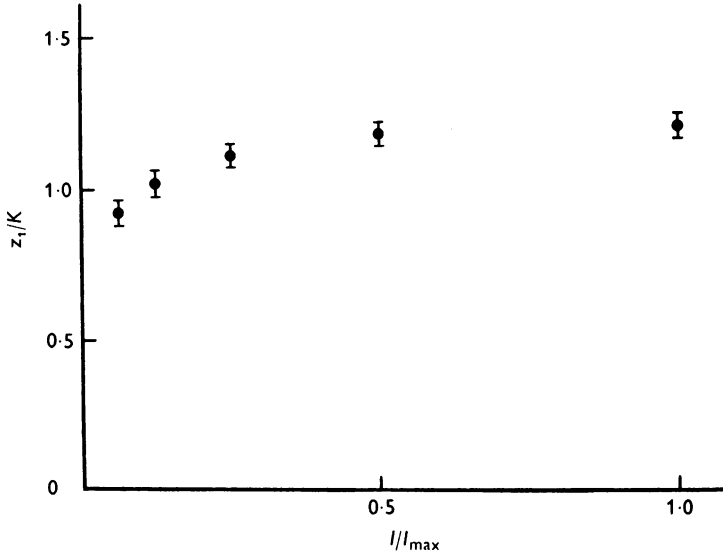
We can reach the same conclusion by analysing the plateau of responses to steps of light.

In general the equations describing the removal of blocking particles according to the model of Baylor *et al.* (1974b), are:

$$\dot{z}_1 = \alpha y_5 - k_{12} z_1 + \bar{C} k_{12} z_2, \quad (10)$$

$$\dot{z}_2 = k_{12} z_1 - (\bar{C} k_{12} + k_{23}) z_2 + k_{32} z_3, \quad (11)$$

$$\dot{z}_3 = k_{23} z_2 - (k_{32} + k_{34}) z_3, \quad (12)$$



Text-fig. 15. Relation between z_1/K , derived at the plateau of responses to flashes, and light intensity. In the ordinates z_1/K is computed with eqn. (6) from data of Text-fig. 14, 1.2 sec after the onset of the flash. In the abscissa the light intensity is given as a fraction of I_{\max} where I_{\max} is the intensity of the unattenuated light.

where the degradation of Z_1 into Z_2 is autocatalytic according to:

$$k_{12} = \bar{k}_{12} + \nu z_2, \quad (13)$$

where ν is the coefficient of autocatalysis.

At 900 msec after the onset of a step of light, a steady state is reached (see Text-fig. 1).

Then

$$\dot{z}_1 = \dot{z}_2 = \dot{z}_3 = 0$$

and assuming k_{32} sufficiently small eqns. (10–12) yield:

$$\frac{z_1}{K} = \frac{(1 + \bar{Q} I/I_{\max}) P I/I_{\max}}{1 + \bar{R} I/I_{\max}}, \quad (14)$$

where

$$\bar{P} = \frac{k_{23} + \bar{C} \bar{k}_{12}}{k_{23} K \bar{k}_{12}} I_{\max}; \quad \bar{Q} = \frac{\bar{C} \nu}{k_{23} (k_{23} + \bar{C} \bar{k}_{12})} I_{\max}; \quad \bar{R} = \frac{\nu}{\bar{k}_{12} k_{23}} I_{\max}. \quad (15)$$

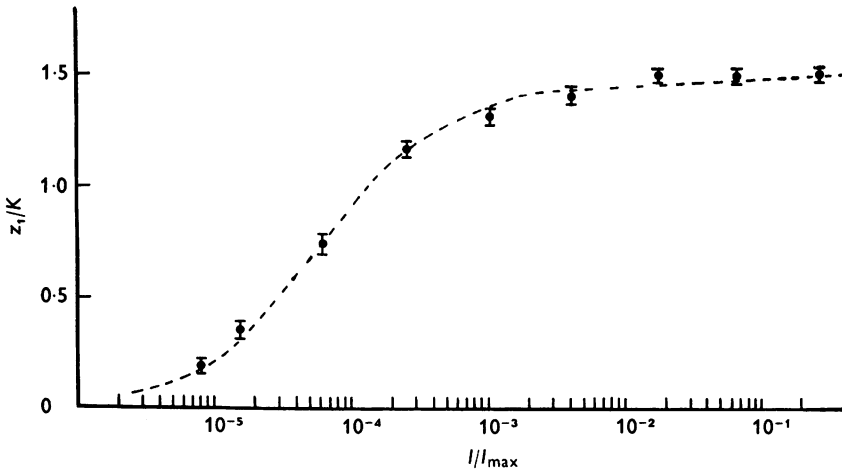
The experimental values of z_1/K at 900 msec after the onset of light are calculated from eqn. (6) and plotted in Text-fig. 16 from the responses shown in Text-fig. 1.

The points are fitted by eqn. (14) with:

$$\bar{P}/I_{\max} = 2.343 \times 10^{-2}; \quad \bar{Q}/I_{\max} = 1.49 \times 10^{-7}; \quad \bar{R}/I_{\max} = 1.61 \times 10^{-2}.$$

Here $\chi_7^2 = 4.35$ and $\bar{\chi}^2 = \frac{\chi_7^2}{7} = 0.62$.

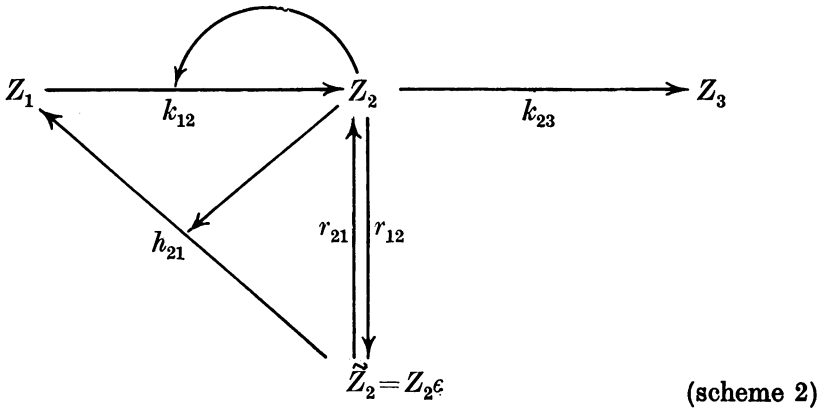
We used the Minit Program (James & Roos, 1973). The fitting was carried out by minimization of χ^2 . At the beginning we used a Monte Carlo searching subroutine; then a minimizing subroutine with the Simplex method by Nelder & Mead (1964) and another one based on a variable metric method (Fletcher & Powell, 1963; Fletcher, 1970). The minimization stopped when a $\chi^2 < 0.8$ was reached.



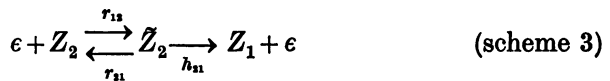
Text-fig. 16. Relation between z_1/K calculated from eqn. (6) at the plateau of responses to steps of light. As in Text-fig. 15 the light intensity is given in fractions of I_{\max} . Plotted data are from the experiment of Text-fig. 1 calculated 0.9 sec after the beginning of the step. The broken line is derived from eqn. (14) with the values of \bar{P} , \bar{Q} , \bar{R} , as stated in the text.

By substitution of the numerical values of \bar{Q} and \bar{R} in eqn. (14), as $\bar{k}_{12} = 10 \text{ sec}^{-1}$ and k_{23} of the same order of $1/\tau \simeq 1 \text{ sec}^{-1}$ (see p. 20), it results in: $\bar{C} \simeq 10^{-6}$, a value incompatible with the observed duration of the plateau.

As a consequence of the above considerations we tried to account for the desensitization of g_1 assuming that the conversion of Z_2 back to Z_1 occurs through a rate limiting enzymatic reaction, as shown in the following scheme.



Here $\tilde{Z}_2 = Z_2\epsilon$ is the active substrate-enzyme complex; ϵ is the enzyme and h_{21} , r_{12} , r_{21} are rate constants. For simplicity we suppose that $k_{12}/h_{21} = D_1$ where D_1 is a constant. Thus for the conversion of Z_2 into Z_1 we have the following scheme:



and the equations:

$$\dot{z}_2 = -r_{12}z_2(e-s) + r_{21}s, \quad (16)$$

$$\dot{s} = r_{12}z_2(e-s) - (r_{21} + h_{21})s, \quad (17)$$

where e is the total concentration of the enzyme, s is the concentration of \tilde{Z}_2 ; r_{12} , r_{21} and h_{21} are the rates of the reactions shown in scheme (3). If we suppose that \tilde{Z}_2 is in a state of near-equilibrium (that is r_{12} and r_{21} are large as compared to the other rates of reaction), eqn. (17) for $\dot{s} = 0$, yields:

$$s = \frac{z_2 e}{d + z_2}; \quad d = \frac{r_{21} + h_{21}}{r_{12}} \simeq \frac{r_{21}}{r_{12}}. \quad (18)$$

Using eqn. (18), eqn. (16) becomes:

$$\dot{z}_2 = -\frac{k_{12} \gamma z_2}{1 + \beta z_2}, \quad (19)$$

where

$$\gamma = \frac{e}{dD_1}, \quad \beta = \frac{1}{d},$$

maintaining the hypothesis that the conversion of Z_1 into Z_2 is autocatalysed by Z_2 (eqn. 13), the rate of the backward reaction k_{21} is given by:

$$k_{21} = \frac{(\bar{k}_{12} + \nu z_2) \gamma}{1 + \beta z_2}. \quad (20)$$

Thus according to schemes (2) and (3), k_{21} grows with z_2 when z_2 is small and saturates at values of $\nu\gamma/\beta$. From this hypothesis it follows that at the plateau of response to a step:

$$z_1 = \frac{\gamma z_2}{1 + \beta z_2}, \tag{21}$$

We then have:

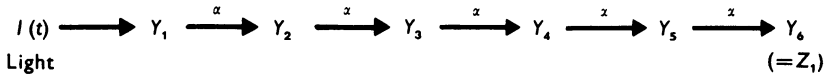
$$\frac{z_1}{K} = \frac{PI(1+QI)}{1+RI+SI^2} \tag{22}$$

with:

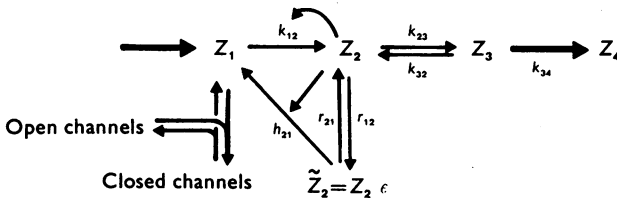
$$P = \frac{k_{23} + \gamma \bar{k}_{12}}{K \bar{k}_{12} k_{23}}; \quad Q = \frac{\beta k_{23} + \nu \gamma}{k_{23} (k_{23} + \gamma \bar{k}_{12})}; \quad R = \frac{\nu + \beta \bar{k}_{12}}{\bar{k}_{12} k_{23}}; \quad S = \frac{\nu \beta}{K k_{23}^2}.$$

The experimental value of z_1/K calculated at the steady state with eqn. (6) from the experimental responses to steps of light are fitted by eqn. (22) with: $P = 5.1606 \times 10^{-2}$; $Q = 5.576 \times 10^{-2}$; $R = 2.255 \times 10^{-1}$; $S = 1.914 \times 10^{-3}$ and I is the light intensity in units such that the unattenuated light is equal to 10^6 .

Build up of particles



Removal of particles



Text-fig. 17. Proposed scheme of the reactions controlling the concentration of the blocking particle. Y is used for indicating the build up of the blocking particle and Z for indicating the removal. The reaction from Z_1 to Z_2 is supposed to be autocatalytic, that is $k_{12} = \bar{k}_{12} + \nu z_2$. The reaction from Z_2 to Z_1 is supposed to be catalysed by Z_2 , that is $h_{21} = k_{12}/D$.

The schemes in Text-fig. 17 summarize our present hypothesis on the build up and on removal of the blocking substance Z_1 .

Reconstruction of rod responses

In what follows the rod responses to a variety of light stimuli computed according to the above model are reported and compared with the

experiments. The equations of the model are summarized in Table 1 and the numerical values of the parameters used are given in Table 2.

The concentration of the substances, Y_1 and Z_1 namely $y_1, \dots, y_5, z_1, z_2, z_3$ are dimensionless. The initial conditions for the integration are

$$y_1(0) = \dots = y_5(0) = z_1(0) = \dots = z_3(0) = 0.$$

The initial conditions for V and h were determined allowing the system to relax in darkness towards the resting value. The system of equations was integrated numerically, using the Runge-Kutta method with variable integration interval δ . The results were checked by decreasing everywhere δ by at least a factor of 10. Calculations were carried out at the Computer Center of the University of Genoa.

TABLE 1. Equations for the reconstruction of the electrical responses of *Bufo marinus* rods

Electrical properties (see Text-fig. 11):

$$C \frac{dV}{dt} = (E_1 - V)\bar{g} + (g_t + g_i)(E_2 - V),$$

$$g_i = \frac{\bar{g}_i}{1 + z_1/K},$$

$$g_t = \bar{g}_t h^3; \quad \frac{dh}{dt} = \frac{h_\infty(V) - h}{\tau_h(V)}; \quad h_\infty(V) = \frac{1}{1 + e^{(V - V_t)/V_e}}; \quad \tau_h(V) = \frac{\tau_h(\infty)}{1 + e^{-(V - V_\tau)/V_\eta}}.$$

Here V_t , V_e , V_τ , V_η are parameters which determine the actual shapes of the relations between the potential V and h_∞ and τ_h respectively.

Build up of the blocking substance (see Text-fig. 17):

$$\begin{aligned} \dot{y}_1 &= I(t) - \alpha y_1, \\ \dot{y}_2 &= \alpha y_1 - \alpha y_2, \\ \dot{y}_3 &= \alpha y_2 - \alpha y_3, \\ \dot{y}_4 &= \alpha y_3 - \alpha y_4, \\ \dot{y}_5 &= \alpha y_4 - \alpha y_5. \end{aligned}$$

Removal of the blocking substance (see Text-fig. 17):

$$\begin{aligned} \dot{z}_1 &= \alpha y_5 - (\bar{k}_{12} + \nu z_2) z_1 + (\bar{k}_{12} + \nu z_2) \frac{\gamma z_2}{1 + \beta z_2} \\ \dot{z}_2 &= (\bar{k}_{12} + \nu z_2) z_1 - (\bar{k}_{12} + \nu z_2) \frac{\gamma z_2}{1 + \beta z_2} - k_{23} z_2 + k_{32} z_3, \\ \dot{z}_3 &= -(k_{32} + k_{34}) z_3 + k_{23} z_2. \end{aligned}$$

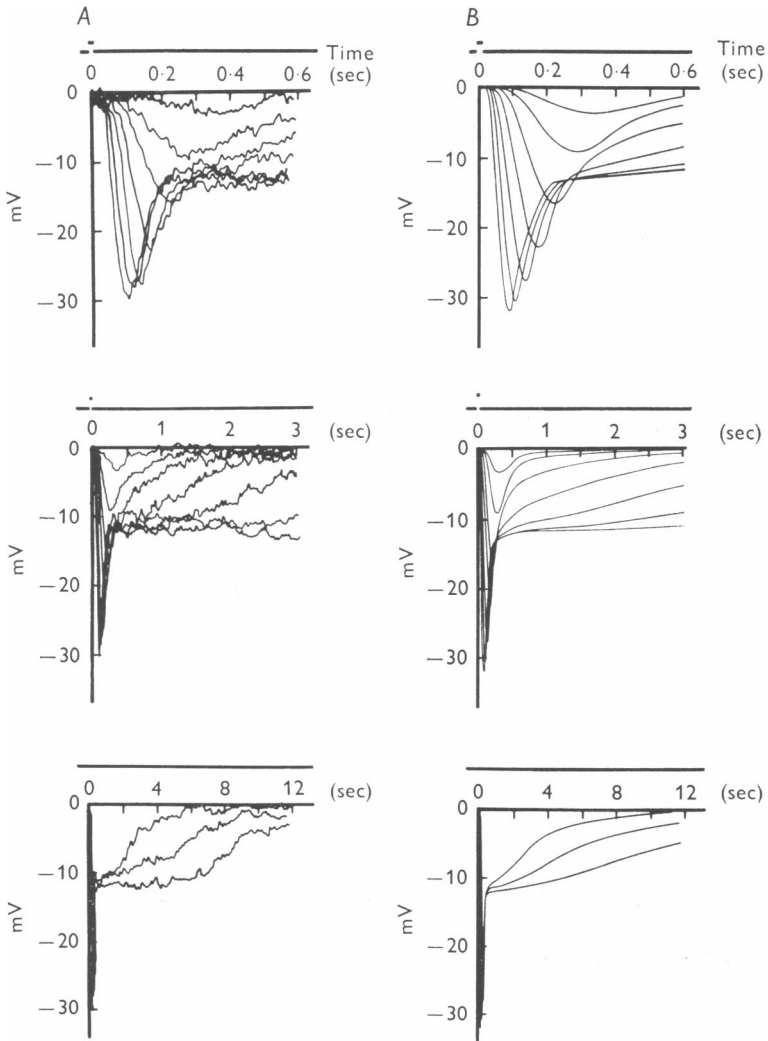
TABLE 2. Values of the parameters adopted to reproduce the experimental responses

Values of the parameters:

$\alpha = 16.6 \text{ sec}^{-1}$	$\bar{k}_{12} = 10 \text{ sec}^{-1}$
$k_{23} = 1.2 \text{ sec}^{-1}$	$k_{34} = 0.27 \text{ sec}^{-1}$
$k_{32} = 0.05 \text{ sec}^{-1}$	$\gamma = 0.035$
$\beta = 0.0106$	$\nu = 2.6 \text{ sec}^{-1}$
$K = 2.5$	$C = 62 \text{ pF}$
$E_1 = 60 \text{ mV}$	$E_2 = 0 \text{ mV}$
$\bar{g} = 3.3 \times 10^{-9} \text{ mho}$	$\bar{g}_i = 7.7 \times 10^{-9} \text{ mho}$
$\bar{g}_t = 4.95 \times 10^{-9} \text{ mho}$	$V_t = -32 \text{ mV}$
$V_e = 1 \text{ mV}$	$\tau_{h(\infty)} = 0.2 \text{ sec}$
$V_\tau = -48 \text{ mV}$	$V_\eta = 4 \text{ mV}$

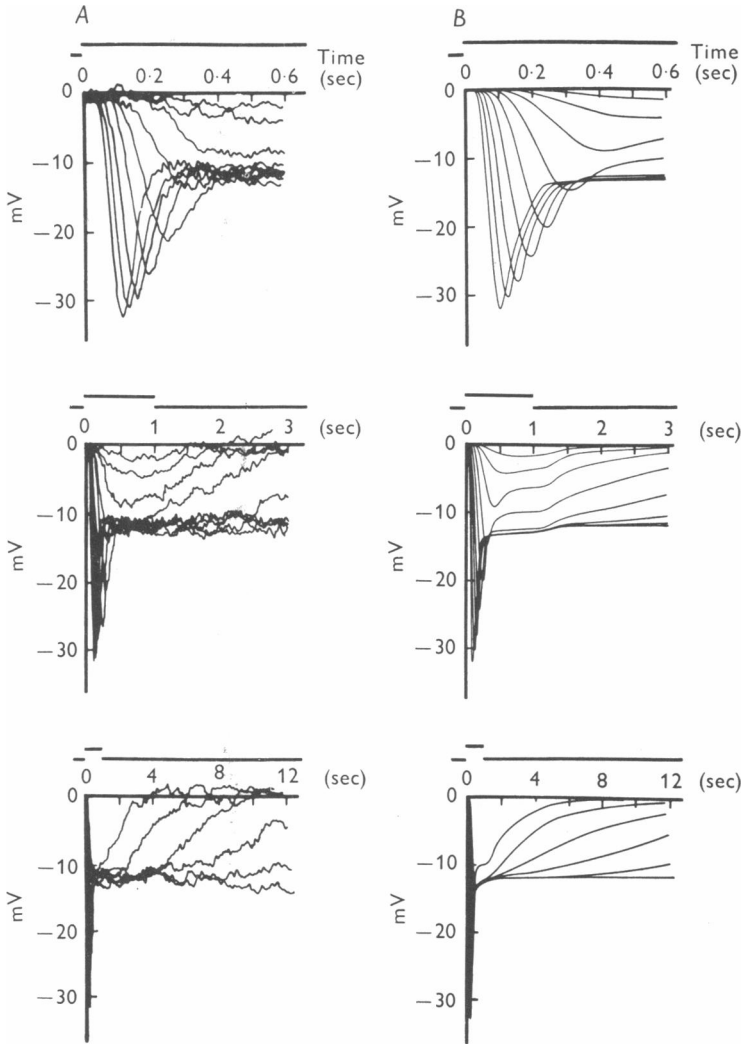
Flashes and steps

Text-fig. 18 illustrates rod responses to flashes of increasing intensity. The experimental results (Text-fig. 18A) are compared on three different time scales with the theoretical curves (Text-fig. 18B) computed according



Text-fig. 18. *A*, comparison at three time scales between responses to flashes of 13 msec of a rod outer segment and *B*, curves computed on the model. Experimental data were obtained with quantities of light increasing by steps of $10^{0.6}$ from an intensity equivalent to $11.2 \text{ photon} \cdot \mu\text{m}^{-2} \cdot \text{sec}^{-1}$ at the wave-length of 510 nm to an intensity equivalent to $2.8 \times 10^4 \text{ photon} \cdot \mu\text{m}^{-2} \cdot \text{sec}^{-1}$. Theoretical curves were computed for lights increasing by steps of $10^{0.6}$ from $10^{2.4}$ to 10^6 units.

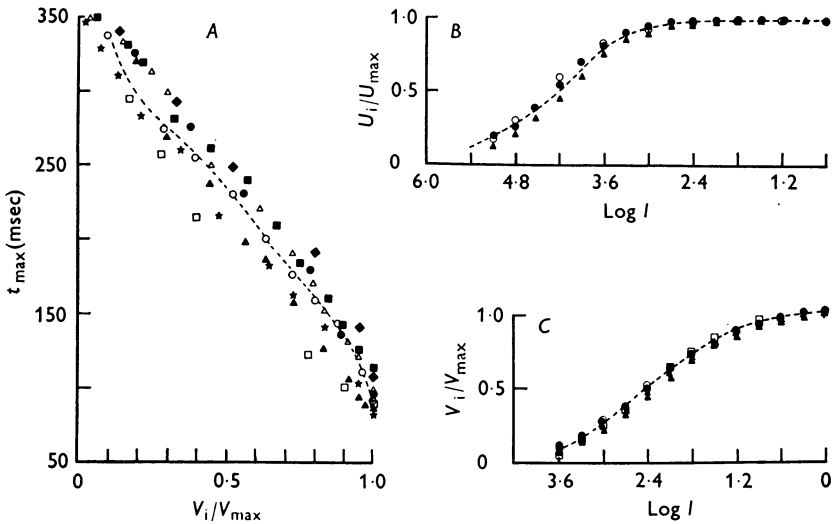
to the model discussed in the previous sections. A similar comparison between experimental (Text-fig. 10A) and computed (Text-fig. 10B) responses is shown in Text-fig. 10, for 1 sec steps of light of increasing intensity. The model reproduces fairly accurately amplitude and temporal



Text-fig. 19. Comparison between experimental and theoretical responses to 1 sec steps on three time scales. *A*, experimental responses were obtained with quantities of light increasing by steps of $10^{0.6}$ from an equivalent intensity at 510 nm of $0.11 \text{ photon} \cdot \mu\text{m}^{-2} \cdot \text{sec}^{-1}$ to $0.7 \times 10^4 \text{ photon} \cdot \mu\text{m}^{-2} \cdot \text{sec}^{-1}$. *B*, theoretical curves were computed for quantities of light increasing by steps of $10^{0.6}$ from $10^{0.6}$ to $10^{5.4}$ units.

features of rod responses to both flashes and steps of light over the entire physiological range. As illustrated by the records reported at slow temporal scales, theoretical curves satisfactorily reproduce the decay of experimental responses also to bright saturating lights when the membrane potential relaxes to the resting level in several seconds.

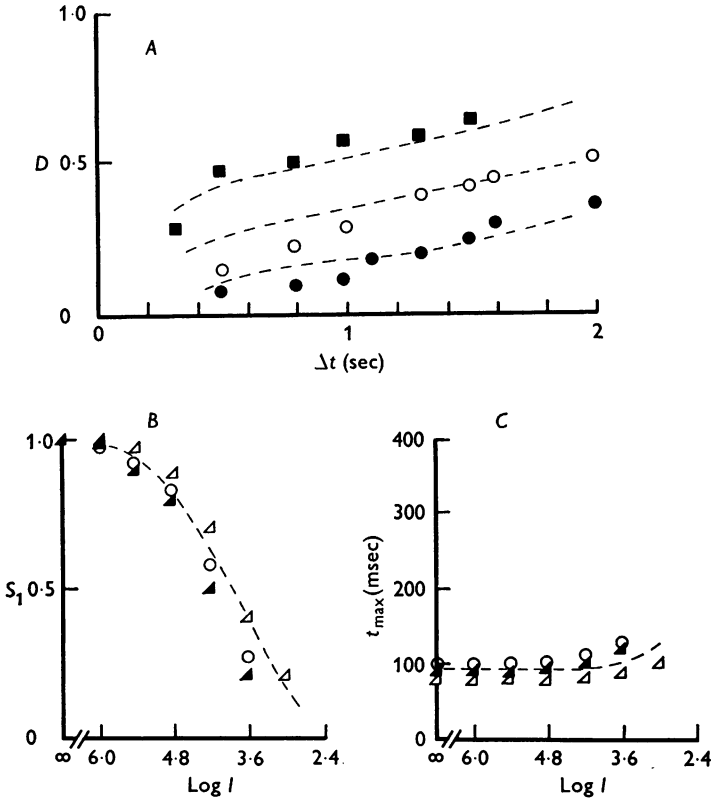
The theoretical relation between amplitude of responses and time-to-peak is compared with data from eight rods in Text-fig. 20*A*. In the same Text-figure the normalized values of the amplitude of the plateau for three rods are plotted against the logarithm of the light intensity in Text-fig. 20*B* and the normalized amplitude of the peak for five rods is plotted in Text-fig. 20*C*. The theoretical relations expressed by the dashed lines provide an excellent fit of the experimental points.



Text-fig. 20. *A*, relation between time-to-peak and normalized amplitude responses to flashes. Experimental data from nine rods. The ordinate is the time to peak from the onset of the flash. The abscissa is the amplitude of the response (V_i) divided by the maximum amplitude with saturating flashes (V_{\max}). The dashed line is the relation derived from the model. *B*, relation between steady hyperpolarization and light intensity for three rods. The ordinate is the amplitude of steady-state response (U_i) 0.9 sec after the onset of a step of light of 1 sec divided by the maximum steady-state response (U_{\max}) with saturating steps. The abscissa is the light attenuation in log. units. The dashed line is the relation derived from the model. *C*, relation between normalized peak amplitude response and intensity of flash for five rods. The ordinate is the amplitude of the response divided by the maximum amplitude with saturating flashes. In abscissa is the light attenuation in log. units. The dashed line is the relation derived from the model.

Pairs of flashes with different time intervals

In a previous section we have analysed the properties of temporal resolution of rods by illuminating the receptor with paired flashes of several intensities delivered at different time intervals Δt . We showed that the effect of the first flash on the response to the second one depends on the



Text-fig. 21. *A*, relation between D and Δt . The experimental data are from three light intensities:

$$\frac{V_i}{V_{\text{max}}} = 0.51, \blacksquare; \quad \frac{V_i}{V_{\text{max}}} = 0.78, \circ; \quad \frac{V_i}{V_{\text{max}}} = 0.98, \bullet.$$

The dashed lines are the relations between D and Δt derived from the theory for the three given intensities. *B*, relation between S_1 and light intensity of the background. The experimental data are from responses to bright flashes ($V_i/V_{\text{max}} = 0.98$) for three rods. The dashed line is the same relation derived from the theory. *C*, relation between time-to-peak and light intensity of the background. The experimental data are from responses to bright flashes ($V_i/V_{\text{max}} = 0.99$) for three rods. The dashed line is the same relation derived from the theory.

light intensity and on Δt , the temporal resolution decreasing as the intensity of the light is increased.

In Text-fig. 21A the theoretical relations (dashed lines) between the quantity D , defined on page 22, and Δt is compared with experimental data for three values of V_i/V_{\max} from the same rod. The agreement between experimental and computed results is satisfactory in the whole range of light intensities used.

Flashes on backgrounds

The most evident effect of a conditioning background is to reduce the amplitude of the response to a flash superimposed on it. The dashed curve in Text-fig. 21B is a theoretical plot of the ratio, S_1 , between A_1 , the amplitude of the peak of a response to a bright flash ($V_i/V_{\max} = 0.98$) superimposed on the background and A_2 , the amplitude of the response to the same flash in dark adapted conditions, against the intensity of the background. It is seen that the model reproduces fairly accurately the experimental results obtained from three different cells.

As to the effect of the background on the temporal scale of the response the model reproduces the experimental data. This is shown in Text-fig. 21C where the change in time-to-peak for a bright flash ($V_i/V_{\max} = 0.98$) is plotted against the intensity of background. The present data obtained by superimposing a flash on backgrounds of light refer only to responses to bright flashes, a condition in which the quantities S_1 and t_{\max} could be most accurately measured. We did not explore the effect of background on responses to flashes covering the entire physiological range.

DISCUSSION

The validity of the model for *Bufo marinus* rods that we have described in the present paper was checked only for the outer segment of the visual cell. Experimental evidence indicates that more complicated events might take place at the inner segment where special properties of the membrane are thought to produce also some kind of amplification (Werblin, 1975).

The present model follows the main framework of the theory proposed for the turtle cone (Baylor *et al.* 1974a, b) and it shares its limitations. The most important change has been introduced to account for the pronounced sag of the response to a plateau, always occurring in a range of membrane potentials where the rod displays still a fairly ohmic behaviour. We suppose that the sag from the peak to the plateau is caused by an increase in the light dependent conductance, rather than to a delayed increase of a voltage dependent conductance. Therefore, during the plateau of responses to saturating flashes and steps of light, a significant fraction of light sensitive

channels are expected to be open in our model while all the channels in the model for turtle cones (Baylor *et al.* 1974*a, b*) are expected to be closed. Peak transient conductance changes followed by a plateau have been measured in photoreceptors of invertebrates (Brown *et al.* 1970; Millecchia & Mauro, 1969*a, b*) where the shape of the response to light closely resembles rod responses with inverted polarity.

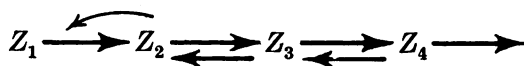
It seems reasonable to identify the battery E_1 of Text-fig. 11 with the K^+ equilibrium potential and the battery E_2 with the Na^+ equilibrium potential. However, since E_2 is nearly zero, one would have to assume that the external concentration of free Na^+ is close to that of the intracellular space.

As to the molecular events responsible for the desensitization of the light dependent conductance, we favour the enzymatic reaction. The reason for the choice is that such a mechanism is relatively simple and commonly observed in biochemical phenomena. Since enzymes are expected to accelerate both forward and backward reactions equally, an implicit assumption of scheme (2), where the reaction from Z_1 to Z_2 and the one from Z_2 to Z_1 are unidirectional, is that either one must be coupled to some parallel exergonic process. It has been shown recently (Robinson, Yoshikami & Hagens, 1975; Carretta & Cavaggioni, 1976), that break-down of high energy phosphate esters occurs in the rod outer segments after illumination but it is not established whether or not this energy is used in the early phase of the phototransduction.

The energy required by the model could actually be fed into the system in many ways. If one makes the hypothesis that the Ca^{2+} ion is the internal transmitter, Z_1 could be identified with free intracellular Ca^{2+} leaked out from the disks after illumination. In this case the removal of the blocking particle could be easily viewed as part of the process of active transport of Ca^{2+} inside the disks and conceivably the reaction from Z_1 to Z_2 could use up some of the energy required by such process.

Alternatively, energy could be introduced in the reaction from Z_2 to Z_1 , if Z_2 were interpreted as Ca^{2+} , chelated by some agent, which needs energy to be freed from the chelating molecules.

A model for the rod in which metabolic energy is required only when the photoresponse is over could also be worked out with the introduction of additional parameters. For instance, one could suppose the following scheme for the removal of the blocking particles:



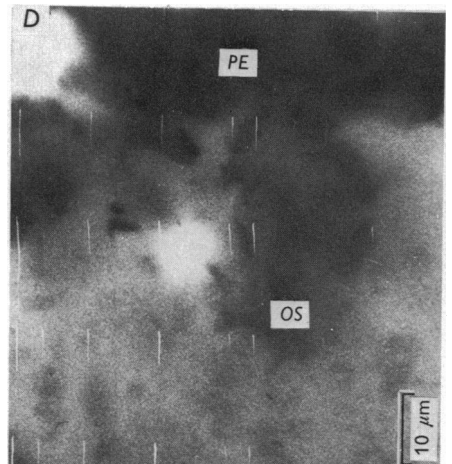
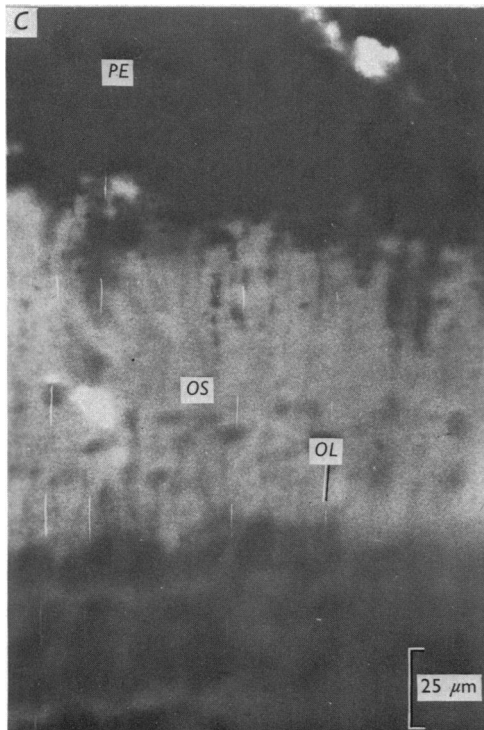
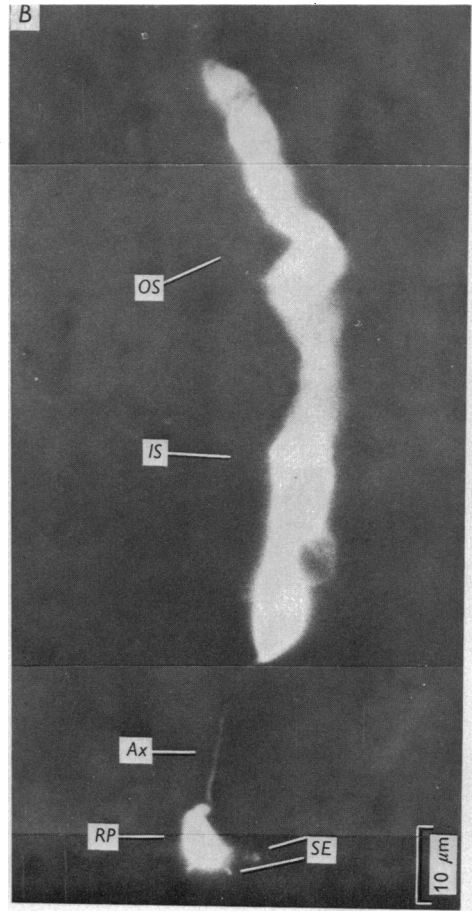
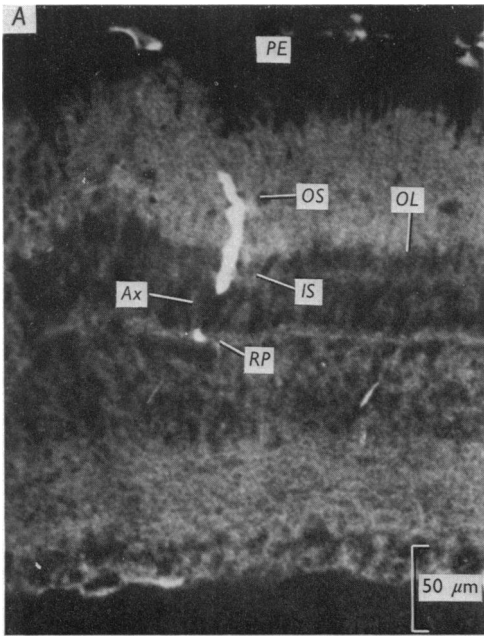
and assuming the existence of two types of channels, a fraction n_1 which can be blocked only by Z_1 and a fraction n_2 which can be blocked by both Z_1 and Z_2 . In this case the peak of the photoresponse would be controlled by Z_1 , while the plateau would be maintained by Z_2 .

We are deeply indebted to Drs M. G. F. Fuortes and F. Conti for the generous help in discussing data and preparing the manuscript. We thank Professor A. L. Hodgkin for critical reading of the manuscript. The helpful suggestions of Dr A. Cavagioni and the technical assistance of Mr G. Bottaro are also acknowledged.

REFERENCES

- BAYLOR, D. A. & FUORTES, M. G. F. (1970). Electrical responses of single cones in the retina of the turtle. *J. Physiol.* **207**, 77–92.
- BAYLOR, D. A. & HODGKIN, A. L. (1973). Detection and resolution of visual stimuli by turtle photoreceptors. *J. Physiol.* **234**, 163–198.
- BAYLOR, D. A. & HODGKIN, A. L. (1974). Changes in time scale and sensitivity in turtle photoreceptors. *J. Physiol.* **242**, 729–758.
- BAYLOR, D. A., HODGKIN, A. L. & LAMB, T. D. (1974*a*). The electrical response of turtle cones to flashes and steps of light. *J. Physiol.* **242**, 685–727.
- BAYLOR, D. A., HODGKIN, A. L. & LAMB, T. D. (1974*b*). Reconstruction of the electrical responses of turtle cones to flashes and steps of light. *J. Physiol.* **242**, 759–791.
- BORTOFF, A. & NORTON, A. L. (1967). An electrical model of the vertebrate photoreceptor cell. *Vision Res.* **7**, 253–263.
- BROWN, H. M., HAGIWARA, S., KOIKE, H. & MEECH, R. M. (1970). Membrane properties of a barnacle photoreceptor examined by the voltage clamp technique. *J. Physiol.* **208**, 385–413.
- BROWN, J. E. & PINTO, L. H. (1974). Ionic mechanism for the photoreceptor potential of the retina of *Bufo marinus*. *J. Physiol.* **236**, 575–591.
- CARRETTA, A. & CAVAGGIONI, A. (1976). On the metabolism of the rod outer segments. *J. Physiol.* **257**, 687–697.
- CAVAGGIONI, A., SORBI, R. T. & TURINI, S. (1973). Efflux of potassium from isolated rod outer segments: a photic effect. *J. Physiol.* **232**, 609–620.
- CERVETTO, L. (1973). Influence of sodium, potassium and chloride ions on the intracellular responses of turtle photoreceptors. *Nature, Lond.* **241**, 401–403.
- COPENHAGEN, D. R. & OWEN, W. G. (1976). Coupling between rod photoreceptors in a vertebrate retina. *Nature, Lond.* **260**, 57–59.
- CRESCITELLI, F. (1972). The visual cells and visual pigments of the vertebrate eye. In *Handbook of Sensory Physiology*, vol. 7, part 1, *Photochemistry of Vision*, ed. DARTNALL, H. T. A., pp. 245–353. New York: Springer-Verlag.
- DARTNALL, H. T. A. (1968). The photosensitivities of visual pigments in the presence of hydroxylamine. *Vision Res.* **8**, 339–358.
- FAIN, G. L. (1975). Quantum sensitivity of rods in the toad retina. *Science, N.Y.* **187**, 838–841.
- FLETCHER, R. & POWELL, M. J. D. (1963). A rapidly convergent descent method for minimization. *Comput. J.* **6**, 163–168.
- FLETCHER, R. (1970). A new approach to variable metric algorithms. *Comput. J.* **13**, 317–329.
- FRANK, K. & FUORTES, M. G. F. (1956). Stimulation of spinal motoneurons with intracellular electrodes. *J. Physiol.* **134**, 451–470.

- FUORTES, M. G. F. & HODGKIN, A. L. (1964). Changes in time scale and sensitivity in the ommatidia of *Limulus*. *J. Physiol.* **172**, 239–263.
- HAGINS, W. A., PENN, R. D. & YOSHIKAMI, S. (1970). Dark current and photocurrent in retinal rods. *Biophys. J.* **10**, 380–412.
- HÁROSI, F. I. (1975). Absorption spectra and linear dichroism of some amphibian photoreceptors. *J. gen. Physiol.* **66**, 357–382.
- HODGKIN, A. L. & HUXLEY, A. F. (1952). A quantitative description of membrane current and its application to conduction and excitation in nerve. *J. Physiol.* **117**, 500–544.
- JAMES, F. & ROOS, M. (1973). *Minuit Program Library*, Geneva; CERN Computer Centre.
- KORENBROT, J. T. & CONE, R. A. (1972). Dark ionic flux and the effects of light in isolated rod outer segments. *J. gen. Physiol.* **60**, 20–45.
- LASANSKY, A. & MARCHIAFAVA, P. L. (1974). Light-induced resistance changes in retinal rods and cones of the Tiger salamander. *J. Physiol.* **236**, 171–191.
- MCALLISTER, R. E., NOBLE, D. & TSIEN, R. W. (1975). Reconstruction of the electrical activity of cardiac Purkinje fibres. *J. Physiol.* **251**, 1–59.
- MILLECCHIA, R. & MAURO, A. (1969*a*). The ventral photoreceptor cells of *Limulus*. II. The basic photoresponse. *J. gen. Physiol.* **54**, 310–330.
- MILLECCHIA, R. & MAURO, A. (1969*b*). The ventral photoreceptor of the *Limulus*. III. The voltage-clamp study. *J. gen. Physiol.* **54**, 331–351.
- NAKA, K.-I. & RUSHTON, W. A. H. (1966). S-potentials from colour units in the retina of fish (*Cyprinidae*). *J. Physiol.* **185**, 536–555.
- NELDER, J. A. & MEAD, R. (1964). A simplex method for function minimization. *Comput. J.* **13**, 317–329.
- ROBINSON, W. E., YOSHIKAMI, S. & HAGINS, W. A. (1975). ATP in retinal rods. *Biophys. J.* **15**, 168a.
- RODIECK, R. W. (1973). *The Vertebrate Retina*, pp. 141–143. San Francisco: W. H. Freeman.
- SCHWARTZ, E. A. (1973). Responses of single rods in the retina of the turtle. *J. Physiol.* **232**, 503–514.
- SCHWARTZ, E. A. (1975). Cones excite rods in the retina of the turtle. *J. Physiol.* **246**, 639–651.
- TOYODA, J., HASHIMOTO, H., ANNO, H. & TOMITA, T. (1970). The rod response in the frog as studied by intracellular recording. *Vision Res.* **10**, 1093–1100.
- TOYODA, J., NOSAKI, H. & TOMITA, T. (1969). Light-induced resistance changes in single photoreceptors of *Necturus* and *Gekko*. *Vision Res.* **9**, 453–463.
- WALLS, G. L. (1963). *The Vertebrate Eye and Its Adaptive Radiation*, pp. 598–600. New York: Hafner Publishing.
- WERBLIN, F. S. (1975). Regenerative hyperpolarization in rods. *J. Physiol.* **244**, 53–81.
- ZUCKERMAN, R. (1971). Mechanisms of photoreceptor current generation in light and darkness. *Nature, New Biol.* **234**, 29–31.



EXPLANATION OF PLATE

A, rod cell injected with Procion yellow after recording typical hyperpolarizing photoresponses. In this cell, injection of depolarizing currents increased the amplitude of the photoresponse, in the same way as shown in Text-fig. 10. The cell is completely stained except the distal part of the outer segment. After injection, the retina was kept alive for 45 min to allow dye diffusion. *PE*, pigment epithelium; *OS*, outer segment; *OL*, outer limiting membrane; *IS*, inner segment; *Ax*, axon; *RP*, rod pedicle.

B, the same rod shown in *A* at a greater enlargement. *SE*, synaptic ending.

C and *D*, two localized markings in the region of the rod outer segment layer. At this level responses were similar to those shown in Text-fig. 1. In these cells injection of depolarizing currents decreases the amplitude of photoresponse, in the same way as shown in Text-fig. 6. Retinae were fixed immediately after injection of dye in order to identify the region within the cell, from where responses originated.